

## Pressure Dependence of $^{71}\text{Ga}$ and $^{197}\text{Au}$ Nuclear Magnetic Resonance in Pure and Pd-Doped $\text{AuGa}_2$ <sup>†</sup>

H. T. Weaver, J. E. Schirber, and A. Narath

Sandia Laboratories, Albuquerque, New Mexico 87115

(Received 2 July 1973)

Nuclear-magnetic-resonance measurements have been made of the Knight shift  $K$  and spin-lattice relaxation time  $T_1$  of  $^{71}\text{Ga}$  in  $\text{Au}_{1-x}\text{Pd}_x\text{Ga}_2$  for  $x = 0.0, 0.012,$  and  $0.026$  as a function of hydrostatic pressure to 8.4 kbar and temperature  $T$  in the range 4–300°K. The Knight shift for  $^{197}\text{Au}$  in  $\text{AuGa}_2$  was also measured as a function of pressure at 4°K. Large increases for both the  $^{71}\text{Ga}$  shift and relaxation rate of  $\text{AuGa}_2$  were observed at 4°K near 7 kbar pressure. The magnitudes of  $K$  and  $(T_1T)^{-1}$  exhibited a decrease upon increasing  $T$  at high pressure. In contrast, the  $^{197}\text{Au}$  shift showed both pressure and temperature independence. The  $^{71}\text{Ga}$  Korringa product ( $K^2T_1T$ ) was temperature and pressure dependent and provides evidence of appreciable electron-electron interactions at low temperatures. Increases for  $K$  and  $(T_1T)^{-1}$  were also found at 4°K in Pd-doped  $\text{AuGa}_2$ . Compared to pure  $\text{AuGa}_2$ , the “turn on” occurred at lower pressures and was more gradual, and the magnitude of the effect was smaller. We have interpreted these effects in terms of a band-structure-electron-transition picture, which involves a sharp peak in the density of states located 10–15 meV below the Fermi level at normal volume and absolute zero.

### I. INTRODUCTION

A wealth of experimental data on the intermetallic compounds  $\text{AuGa}_2$ ,  $\text{AuIn}_2$ , and  $\text{AuAl}_2$  has been reported in the recent literature. These materials crystallize in the fluorite structure and have been shown to exhibit valence-7 nearly-free-electron-like behavior in many of their properties. Their magnetic properties have been investigated as a function of Pd doping,<sup>1</sup> of alloying of the compounds with each other,<sup>2</sup> and as a function of temperature through the melting points of the materials.<sup>3</sup> New Fermi-surface information has been obtained using high-field magnetoresistance<sup>4</sup> and de Haas-van Alphen techniques.<sup>5,6</sup> Optical<sup>7</sup> and elastic-constant<sup>8</sup> data as a function of temperature have been reported. The Fermi surface<sup>9</sup> and the superconducting properties<sup>10,11</sup> have been studied as a function of Pd doping and hydrostatic pressure.

Much of this experimental work was stimulated by the magnetic-resonance and susceptibility study of Jaccarino *et al.*,<sup>12</sup> hereafter referred to as JWWM. These workers pointed out that  $\text{AuGa}_2$  has surprisingly different magnetic properties from  $\text{AuIn}_2$  and  $\text{AuAl}_2$ , even though many of the electronic properties, such as the Fermi-surface topologies, the electronic specific heats, and Hall coefficients, are very similar in all three compounds. The most striking anomaly is perhaps the Ga Knight shift, which is observed to change from a positive value of +0.55% near room temperature to -0.13% at liquid-He temperatures. The corresponding Al and In shifts in the other two compounds, as well as the Au Knight shifts<sup>13</sup> in all three compounds, are nearly temperature independent. Anomalies between room temperature and

4°K were also noted in the Ga spin-lattice relaxation rate and in the bulk susceptibility of  $\text{AuGa}_2$ .<sup>12</sup>

JWWM<sup>12</sup> proposed a phenomenological conversion of  $s$  to  $p$  character of the electronic density of states at the Fermi level as the temperature was lowered, to account for the change in sign of the Knight shift. Switendick and Narath<sup>13</sup> were able to account for this behavior within the framework of a physical model based upon the detailed band structures of the three compounds. They found that, while the second band in  $\text{AuAl}_2$  and  $\text{AuIn}_2$  intersects the Fermi level in a roughly free-electron manner, the corresponding band in  $\text{AuGa}_2$  is extremely flat (therefore has a high associated density of states) and lies entirely below the Fermi level. Furthermore, this second band was found to have Ga, In, or Al  $s$  character in the respective compounds. This “missing  $s$  band” situation is consistent with both the original<sup>14</sup> and more recent<sup>5,6</sup> de Haas-van Alphen Fermi-surface studies and with pressure studies of the Fermi surface.<sup>9,15</sup> Switendick and Narath<sup>13</sup> proposed that the anomalous temperature dependence of the magnetic properties of  $\text{AuGa}_2$  stemmed from depopulation of this flat band as the temperature increases, either due to volume effects via thermal expansion or to thermal depopulation.

Schirber and Switendick<sup>15</sup> found that their pressure-dependent Fermi-surface cross-section data agreed with their volume-dependent band-structure calculation. They were able to show by inference from the behavior of the pressure derivatives of the second-zone cross sections in  $\text{AuAl}_2$  and  $\text{AuIn}_2$  and from the calculated band structures that the thermal-expansion contribution was of the wrong sign to depopulate the  $\text{AuGa}_2$  second band. Subse-

quent pressure studies to higher pressures<sup>9</sup> disclosed an anomaly in the behavior of a small cross section of the third zone of the AuGa<sub>2</sub> Fermi surface. Schirber<sup>9</sup> proposed that this behavior was a reflection of the abrupt change in the density of states at the Fermi level as the *second* band passed through the Fermi level from below at about 6 kbar. Such a creation of a new sheet of the Fermi surface is known as an "electron" or "Lifshitz" transition<sup>16</sup> and should result in changes in any electronic property sensitive to the density of states at the Fermi level.

Measurements of the superconducting transition temperature by Schirber<sup>10</sup> as a function of pressure showed a very large and abrupt increase in  $T_c$  at the same pressure as indicated by the Fermi surface work, demonstrating a large increase in the density of states near the Fermi level. (The Pd-doping experiments of Wernick *et al.*<sup>1</sup> had indicated a lesser but still substantial increase in  $T_c$  with increasing Pd content, consistent with the picture of a flat band located below  $E_F$  at zero Pd concentration.) Our measurements<sup>17</sup> of the pressure dependence of the Ga Knight shift and spin-lattice relaxation time in AuGa<sub>2</sub> further substantiated this band-structure-electron-transition picture by showing that this density-of-states peak had substantial Ga s character.

The purpose of this paper is to present low-temperature data on the pressure dependences of the <sup>71</sup>Ga Knight shifts and spin-lattice relaxation rates in Pd-doped AuGa<sub>2</sub> and the <sup>197</sup>Au shift in AuGa<sub>2</sub>, and to correlate the new results with our earlier work. We will consider both the observed pressure and temperature dependences in terms of the band-structure-electron-transition picture and attempt to show that this model can provide a consistent framework for understanding most of the phenomena observed.

In Sec. II we describe our experimental procedures. The techniques used to obtain NMR data to 9 kbar at liquid-He temperatures are described briefly. Our experimental results are given in Sec. III. These results are discussed in Sec. IV, which is subdivided into sections on the Knight shift, spin-lattice relaxation time, Korringa product, and susceptibility. In Sec. V, we summarize our conclusions.

## II. EXPERIMENTAL

The samples were prepared from the same single-crystal material used in the superconductivity and de Haas-van Alphen studies.<sup>9,15</sup> These boules were grown by the Bridgman-Stockbarger technique in fused-silica crucibles in an argon atmosphere. The Pd concentrations were determined by atomic-absorption spectroscopy on portions of the boule adjacent to where the samples were taken.

The samples were prepared by grinding with a mortar and pestle and annealing the <325-mesh powders for ~24 h at 375 °C. The powdered samples were mixed ~3:1 with powdered NaCl to prevent electrical shorting of the particles.

Conventional phase-coherent, single-coil, transient NMR methods were employed, with rotating fields of about 100 Oe. Resonance frequency-to-field ratios were determined for <sup>71</sup>Ga from spin-echo or free-induction profiles as a function of field. The ratios were determined at maximum signal intensity. The <sup>197</sup>Au resonances were much narrower than the <sup>71</sup>Ga resonances, and it was possible to detect interference patterns representing the frequency difference between nuclear and reference signals. Signal averaging was accomplished by a PAR boxcar integrator for the profiles and by a Fabritek multichannel analyzer for the interference patterns.

Spin-lattice relaxation times ( $T_1$ ) were determined from recovery rates of the longitudinal nuclear magnetization following saturation with multiple-pulse trains. Broad lines and rapid relaxation rates near the "transition" in AuGa<sub>2</sub> produced considerable concern regarding the accuracy of  $T_1$ . If the broadening is predominantly due to spatially varying quadrupole interactions, and if saturation of the different transitions is nonuniform, a non-exponential magnetization recovery is expected<sup>18</sup>; more importantly, the initial recovery rate of the central transition is much more rapid than  $T_1^{-1}$ . We checked the broadening mechanism by comparing the linewidths of <sup>71</sup>Ga and <sup>69</sup>Ga, which possess very different quadrupole moments. The linewidths were identical and scaled linearly with applied field. We conclude that the broadening was produced mainly by a spatial distribution of Knight shifts. Thus systematic errors in determining  $T_1$  are believed to be unimportant.

Pressures to ~9 kbar were generated by careful isobaric freezing of He.<sup>19</sup> The rf leads were brought into the high-pressure region through thermocouple leadthroughs sealed with Epoxy similar to those described by Schirber and Shanfeldt.<sup>20</sup> In the present work, the leadthrough was at room temperature and the Epoxy was Eccobond 285 (Emersen and Cuming, Inc.). This mode of operation necessitated using a 45-in. length of the  $\frac{1}{8}$ -in. -i.d. by  $\frac{1}{4}$ -in. -o.d. BeCu high-pressure tubing as the outer conductor of the rf coaxial line leading to the sample coil. Formvar-insulated Cu wire served as the inner conductor. Insulation between the coaxial leads was provided by Teflon spaghetti, which was cut into 4-in. sections to lessen tension on the Cu lead when the Teflon contracted with pressure and cooling.

The high-pressure chamber was a  $\frac{3}{4}$ -in. -o.d. BeCu cylinder with a  $\frac{3}{8}$ -in. -diam  $\times$  1-in. -long

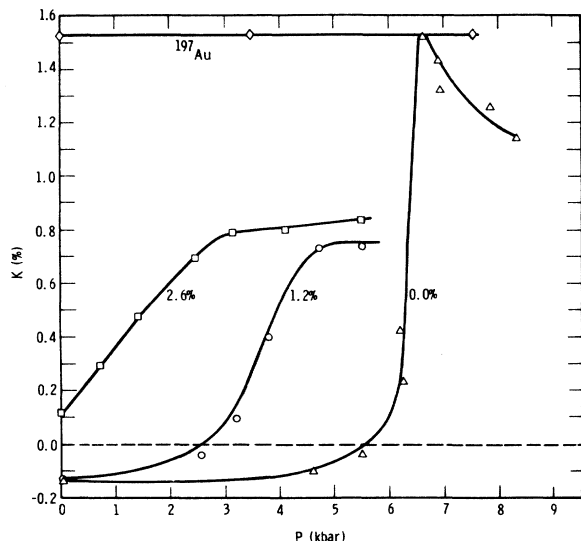


FIG. 1. Pressure dependence of  $^{71}\text{Ga}$  and  $^{197}\text{Au}$  Knight shifts at 4 °K in  $\text{Au}_{1-x}\text{Pd}_x\text{Ga}_2$ . The percentages indicate the value of  $x$ . The  $^{197}\text{Au}$  Knight shift is for  $x = 0$ .

working volume. The closure was a conventional 60° BeCu-to-BeCu cone seal. The  $\frac{7}{16} \times 32$  retaining nut was torqued to 35 ft lb.

Severe ringing<sup>21</sup> of the receiver input, which was attributed to acoustic excitations of the pressure chamber, required that different coil geometries be used for the  $^{71}\text{Ga}$  and  $^{197}\text{Au}$  resonances. The  $^{71}\text{Ga}$  experiments were carried out near 16 kOe (i.e., ~20 MHz) with the sample-coil axis parallel to the axis of the pressure chamber. With this experimental arrangement, a conventional electromagnet could be used to generate the static fields. Even at this relatively high frequency, however, noticeable rf ringing following rf excitation was observed. However, the magnitude and duration of the ringing was such that the nuclear signal could be easily detected. Lowering the frequency to 2 MHz for the  $^{197}\text{Au}$  resonance increased the acoustic signal by several orders of magnitude. The severity of this problem was found to vary with the hardness of the pressure chamber. A minimum occurred for a chamber wall Brinell hardness of 40–42. However, the ringing still persisted for many milliseconds, making observation of the  $^{197}\text{Au}$  NMR in the electromagnet impossible. The resonance frequency of  $^{197}\text{Au}$  was subsequently raised to about 9 MHz with a 140-kOe GE superconducting-magnet system. The solenoidal geometry required that the static magnetic field be parallel to the pressure-chamber axis; thus, a small coil was constructed ( $\frac{1}{8}$ -in.-diam  $\times$   $\frac{1}{8}$ -in. length) with its axis normal to the field. A coil inductance of order 1  $\mu\text{H}$  was achieved by using 28 turns of 0.005-in.-diam wire, so that matching to the re-

ceiver and transmitter was straightforward. At the higher frequency a reduction in the amplitude of the acoustic ringing occurred which allowed detection of the  $^{197}\text{Au}$  spin echo. In both experimental configurations the coils were glued with GE 7031 cement into phenolic holders designed to fill as much of the pressure vessel as possible, thus minimizing the dead volume of the pressure system.

The electromagnet was calibrated using the  $^{195}\text{Pt}$  resonance frequency in Pt metal ( $\nu/H = 0.8783$  kHz/Oe) and the  $^{63}\text{Cu}$  resonance in the coil wire ( $\nu/H = 1.1311$  kHz/Oe). In the solenoid all measurements were made relative to the zero-pressure  $^{197}\text{Au}$  resonance, which was known from previous work.<sup>13</sup> Temperature variation was accomplished simply by immersing the sample in liquid helium, neon, or nitrogen.

### III. RESULTS

The pressure dependence of the Knight shift  $K$  for  $^{71}\text{Ga}$  in  $\text{Au}_{1-x}\text{Pd}_x\text{Ga}_2$  is shown in Fig. 1. With the exception of the low-pressure data, the resonances for  $\text{AuGa}_2$  were 100–200 Oe wide and asymmetric. This asymmetry was especially pronounced near the transition pressure where the tailing off changed from the low-field side below the critical pressure to the high-field side above the critical pressure. As the pressure continued to increase, the resonances became symmetric and somewhat narrower, although the width remained near 100 Oe. Resonances for Pd-doped compounds were broad at all pressures and showed very little change as the Knight shift increased. The  $^{197}\text{Au}$  Knight shift in pure  $\text{AuGa}_2$  is also shown in Fig. 1. We measured the  $^{197}\text{Au}$  shift in  $\text{Au}_{0.95}\text{Pd}_{0.05}\text{Ga}_2$  at atmospheric pressure and 4 °K and found it to be unchanged from the  $\text{AuGa}_2$  value.

Figure 2 shows the temperature dependence of  $K$  for  $^{71}\text{Ga}$  at two pressures. The low-pressure data are from Ref. 12. These data indicate that at low temperature the Fermi energy is at a high density of Ga  $s$  states at 6.9 kbar and at a low density of Ga  $s$  states at zero pressure.

Spin-lattice relaxation rates  $1/T_1T$  for  $^{71}\text{Ga}$  in the three compounds are shown in Fig. 3. Pure  $\text{AuGa}_2$  displays a much larger change with pressure at the transition than the Pd-doped samples. Qualitatively, these data provide the same information as the Knight-shift measurements; however, a nearly-free-electron model does not yield a consistent explanation for the details of the pressure dependence of both  $K$  and  $T_1T$ . We will return to this point later.

The temperature dependence of  $(T_1T)^{-1}$  for  $^{71}\text{Ga}$  in  $\text{AuGa}_2$  at two pressures is shown in Fig. 4. Again the low-pressure data are from Ref. 12. The initial increase of  $(T_1T)^{-1}$  with increasing  $T$

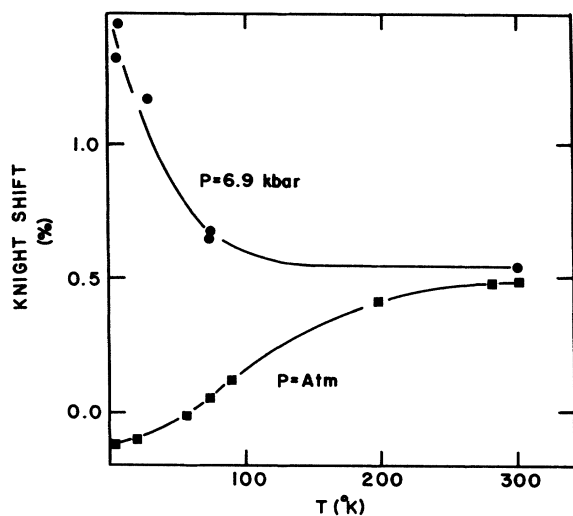


FIG. 2. Temperature dependence of the  $^{71}\text{Ga}$  Knight shift for two pressures, as indicated. The atmospheric-pressure data are from Ref. 12.

was also observed for  $P = 7.5$  kbar.

The pressure dependence of the Korringa product ( $K^2 T_1 T$ ) is shown in Fig. 5. We have plotted the ratio of the calculated product for  $s$  electrons to the experimental value. Usually this ratio ( $\mathcal{K}$ ) provides a measure of electron-electron interactions,<sup>22</sup> but owing to the changing topology of the Fermi surface this interpretation is probably not valid here, as we will discuss in Sec. IV.

#### IV. DISCUSSION

##### A. Knight Shift

In the original paper reporting the temperature dependence of the  $^{71}\text{Ga}$  Knight shift in  $\text{AuGa}_2$ , JWWM proposed a model in which a "metamorpho-

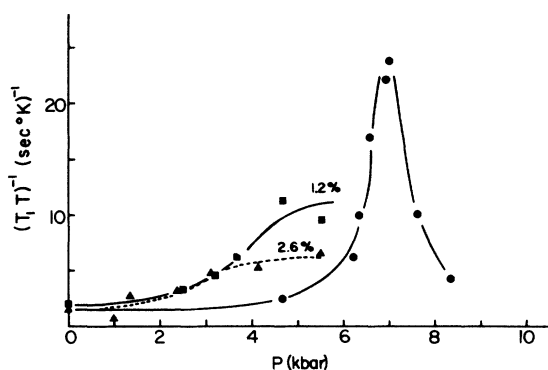


FIG. 3. Pressure dependence of the  $^{71}\text{Ga}$  spin-lattice relaxation rate in  $\text{Au}_{1-x}\text{Pd}_x\text{Ga}_2$ , where  $x$  is indicated by the percentages shown.

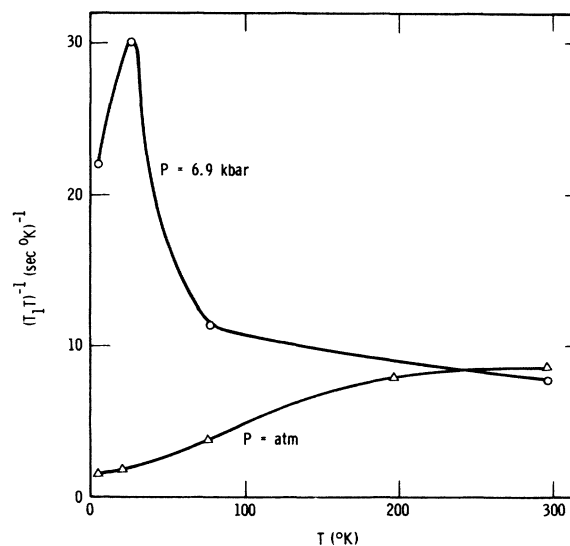


FIG. 4. Temperature dependence of the  $^{71}\text{Ga}$  spin-lattice relaxation rate at two pressures. The atmospheric-pressure data are from Ref. 12.

sis" from  $p$ - to  $s$ -electron character occurred for the conduction electrons as  $T$  increased from 4 to 300  $^\circ\text{K}$ . This postulated change in character was required to provide a consistent interpretation for the temperature dependence of the susceptibility, the  $^{71}\text{Ga}$  spin-lattice relaxation time, and the  $^{71}\text{Ga}$  Knight shift. Since this original work, de Haas-van Alphen experiments<sup>10</sup> have provided rather direct evidence that the amount of  $p$  character at the Fermi level is relatively unchanged for varying conditions of temperature and hydrostatic pressure. The electronic band-structure calculation for  $\text{AuGa}_2$  at normal volume<sup>13</sup> and as a function of interatomic spacing<sup>15</sup> supports this conclusion. Consequently,

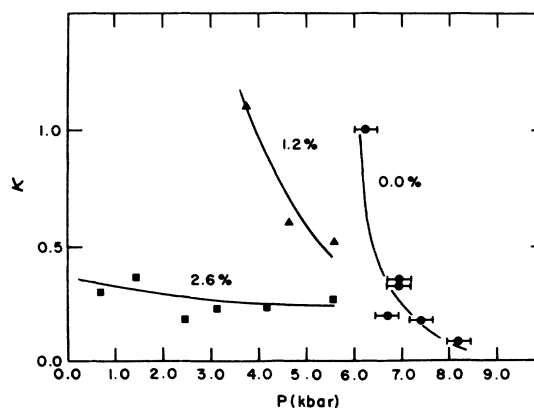


FIG. 5. Pressure dependence of the reciprocal Korringa product for  $^{71}\text{Ga}$  in  $\text{Au}_{1-x}\text{Pd}_x\text{Ga}_2$ , as discussed in text. Values for  $x$  are shown as percentages.

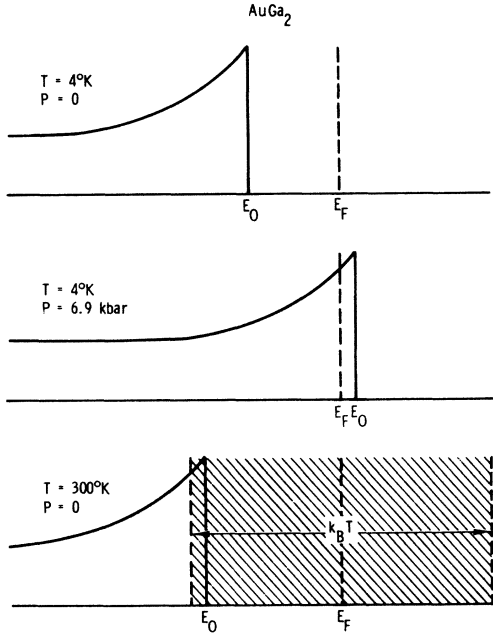


FIG. 6. Schematic representation of relative position of Fermi energy ( $E_F$ ) and the Ga  $s$ -band edge ( $E_0$ ) in  $\text{AuGa}_2$  under varying conditions of temperature and pressure, according to model I. The bottom sketch indicates the energy range sampled in the Knight-shift measurement at 300°K.

our description of the NMR in  $\text{AuGa}_2$  differs from the JWWM model in that the  $p$ -electron contribution is held constant.

Figure 6 schematically illustrates the physical situation we believe to exist in  $\text{AuGa}_2$ . The density of states represented in the figure reflects the flat gallium  $4s$  band which is suggested by the electronic band-structure calculation.<sup>13</sup> Unfortunately, the resolution of the calculation is not fine enough to produce a detailed density-of-states function nor to place the band edge relative to the Fermi energy with sufficient precision to account quantitatively for the various experimental results. For example, in order for the Ga  $s$  electrons to be excited thermally to the Fermi level at  $T \approx 100$ °K, the energy gap must be of order 0.01 eV. We are therefore forced to model the details of the electronic structure, although the basic features are predicted by first-principles considerations.

In our calculations we employ the notation introduced by JWWM and follow the Knight-shift calculation outlined by Warren *et al.*<sup>13</sup> We first write the measured shift as

$$K(T, P) = k_s D(T, P) + k_p (1 - \xi D(T, P)), \quad (1)$$

where  $k_s(k_p)$  is the maximum possible shift due to the  $s$ -electron ( $p$ -electron) character at the Fermi surface and  $D(T, P)$  is a parameter which describes

the temperature and pressure variation of  $K(T, P)$ . The parameter  $\xi$  essentially measures the degree of  $s$  to  $p$  conversion. JWWM used  $\xi = 1$ , but as noted earlier we shall take  $\xi = 0$ . We then set

$$k_p = K(0, 0), \quad (2)$$

$$k_s = K(0, 6.5) - K(0, 0), \quad (3)$$

and use

$$D(T, P) = [K(T, P) - k_p]/k_s \quad (4)$$

to determine  $D(T, P)$  experimentally.

Within the independent-particle approximation<sup>3,23</sup> and assuming an energy-independent hyperfine constant [ $H_{\text{hf}}(s)$ ] we can write

$$K_s(T, P) = k_s D(T, P) = \frac{1}{2} \gamma_e^2 \hbar^2 H_{\text{hf}}(s) \times \left[ \frac{1}{4k_B T} \int_{-\infty}^{+\infty} N_s(E) \text{sech}^2 \left( \frac{E - E_F}{2k_B T} \right) dE \right], \quad (5)$$

where  $E_F$  is the Fermi energy and  $N_s(E)$  is the density of  $s$  states. The remaining terms have their usual meaning. Electron-electron interactions typically enhance  $K_s$  by 20–30% in simple metals.<sup>24</sup> We have accounted for this in our analysis of the Knight shift only to the extent that the enhancement is assumed to be pressure and temperature independent. This assumption is most questionable when  $E_F$  intersects the band edge.

We have carried out calculations using three models for  $N_s(E)$  and the position of the Ga  $s$  band relative to  $E_F$ . In general, we assume

$$N_s(E) = k_s G(E) L, \quad E \leq E_0 \quad (6)$$

$$N_s(E) = 0, \quad E > E_0 \quad (7)$$

where the parameters are defined by the linear approximations

$$E_F - E_0 = A + BP + CT, \quad (8)$$

$$L = \alpha + \beta P. \quad (9)$$

In model I we used the analytical form for  $G(E)$  employed by Smith *et al.*<sup>11</sup> to analyze their superconducting-transition-temperature data.

$$G_I(E) = f + \{(1 + x^2)[(1 + x^2)^{1/2} - x]\}^{-1/2}, \quad (10)$$

where  $x \equiv (E - E_0)/\Gamma$ ,  $f$  is a constant, and the width  $\Gamma$  is taken to be 0.6 mV. For models II and III we used

$$G_{\text{II,III}}(E) = 1, \quad (11)$$

where II differs from III in that  $C \neq 0$  (i.e., the band-edge position  $E_F - E_0$  contains an explicit temperature dependence).

The explicit temperature dependence  $CT$  corresponds to the model suggested by Warren *et al.*,<sup>3</sup> who, however, ignored thermal-expansion effects. In all three models considered here, thermal expansion was taken into account by converting the

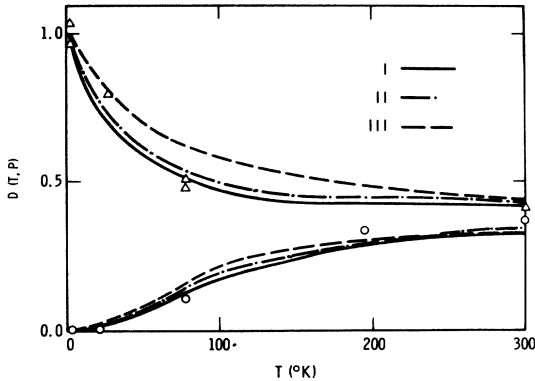


FIG. 7. Comparison of calculated and observed temperature dependence of the fractional  $s$  character, as defined in text. The upper set corresponds to  $P=6.9$  kbar and the lower set to  $P=0$  (i.e., atmospheric pressure).

volume increase relative to that at  $4^\circ\text{K}$  into an equivalent negative pressure. Fits to the experimental temperature dependence of the  $^{71}\text{Ga}$  Knight shift for the 0- and 6.9-kbar isobars are shown in Fig. 7. Using model I we also calculated the pressure dependence of  $D(T, P)$  shown in Fig. 8. The parameters used to calculate these curves are tabulated in Table I.

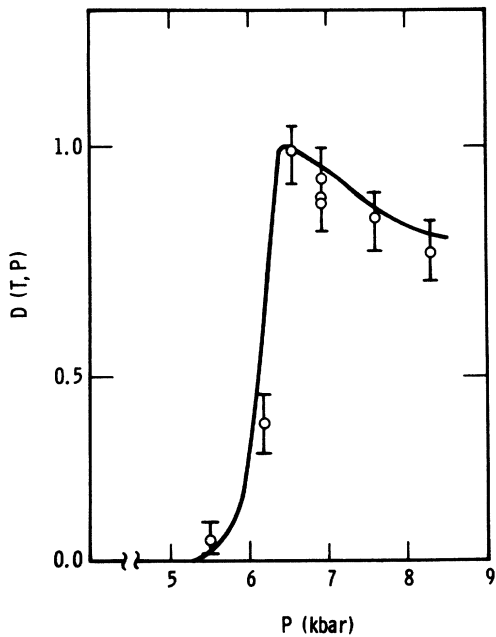


FIG. 8. Comparison of calculated and observed pressure dependences of fractional  $s$  character as defined in text, at  $4^\circ\text{K}$ . The calculated results are based on model I.

TABLE I. Summary of parameters used in model calculations of  $D(T, P)$ .

Model	$A$ (eV)	$B$ (eV/kbar)	$C$ (eV/ $^\circ\text{K}$ )	$\alpha$	$\beta$ (kbar) $^{-1}$	$f$	$\Gamma$ (eV)
I	0.012	-0.002	...	1.2	-0.028	0.5	0.0006
II	0.012	-0.002	...	0.6	-0.014	...	...
III	0.012	-0.002	$4 \times 10^{-5}$	0.5	...	...	...

If we were to use a best-fit criterion to decide between the models, model I would probably be the choice (see Fig. 7). However, the possibility of a variable enhancement of  $K$  requires that some caution be used in this selection. In view of the approximations inherent in the calculations, the fits probably have only semiquantitative significance, so that conclusions relating to the detailed shape of  $N(E)$  are not warranted. Similarly, the possibility of explicit temperature effects is not excluded. On the other hand, the data are explained rather well with model I, and the introduction of additional effects would therefore not seem to be warranted.

In contrast to pure  $\text{AuGa}_2$ , it was not possible to fit the temperature dependence of  $K$  in the Pd-doped samples. All three models produce variations in  $K$  that are much larger and more rapid than observed. It is clear that addition of Pd to  $\text{AuGa}_2$  produces nonrigid-band effects. This is not surprising since the conduction electrons are expected to redistribute so as to screen the Pd charge contrast, producing local variations in the density of states or, equivalently, a smearing of the band edges. The consequences are very pronounced in  $\text{AuGa}_2$  because of the narrow gap between  $E_F$  and the Ga  $s$  band. Additional evidence for nonrigid-band behavior is found in the broad NMR lines in these materials. Line broadening, due to an inhomogeneous  $K$ , directly implies variations in the local density of states. It is interesting to note that the pressure dependence of the superconducting transition temperature was adequately accounted for by Smith *et al.*<sup>11</sup> using the density-of-states function of model I. This disparity can be understood by noting that  $T_c$  is determined by a weighted average of  $N(E)$  over a range of energies within  $k_B\Theta_D$  of the Fermi energy (where  $\Theta_D$  is the Debye temperature), whereas  $K$  only probes a region of width  $k_B T$ . For  $\text{AuGa}_2$ ,  $\Theta_D \approx 200^\circ\text{K}$ , and as a consequence details in  $N(E)$  are much less important in a calculation of  $T_c$  than in a calculation of the low-temperature behavior of  $K$ .

The line broadening which accompanies the transition in pure  $\text{AuGa}_2$  must also be due to an inhomogeneous density of states. However, the cause of the broadening in this case is most likely an inhomogeneous compression of the lattice due to microscopic defects, rather than an intrinsic prop-

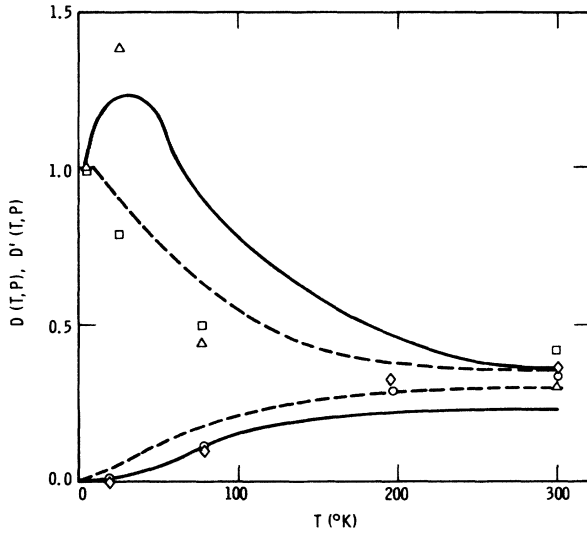


FIG. 9. Comparison of calculated and observed temperature dependences of the fractional  $s$  character as defined in text, calculated from model I using a fit to the  $(T_1 T)^{-1}$  data (solid lines) and  $K$  data (dashed lines). The upper set corresponds to  $P=6.9$  kbar and the lower set to  $P=0$  (i.e., atmospheric pressure). The experimental points which correspond to  $D(T, P)$  are denoted by  $\square$  and  $\diamond$  and to  $D'(T, P)$  by  $\triangle$  and  $\circ$ .

erty of the material. The hydrostatic character of the pressure which is applied to a sample by the solid-helium technique has been demonstrated in a variety of experiments.<sup>25</sup> However, the presence of defects in the lattice allows anisotropy in the response of the sample to the applied pressure. In support of this conjecture, we note that small spatial variations in lattice contraction would cause the pressure-dependent asymmetry in the  $^{71}\text{Ga}$  resonance lines as observed.

#### B. Relaxation Rates

Nuclear spin-lattice relaxation rates in metals are determined by a wave number average of the magnetic response function.<sup>24</sup> Thus, in the presence of electron-electron interactions, the detailed shape of the Fermi surface has a more pronounced effect on  $T_1$  than on  $K$ . In other words, a nearly-free-electron treatment is generally a poorer approximation for  $T_1$  than for  $K$ . The general predictions of the nearly-free-electron model are nevertheless of interest in the  $\text{AuGa}_2$  problem, in that the temperature dependence of  $T_1$  is quite different from that found in the usual high-temperature approximation. In the nearly-free-electron independent-particle approximation, the spin-lattice relaxation rate  $R \equiv (T_1 T)^{-1}$  due to  $s$ -like electrons can be written as<sup>26</sup>

$$R_s(T, P) = \pi k_B \bar{n} \gamma_I^2 H_{\text{hf}}(s)^2$$

$$\times \frac{1}{4k_B T} \int_{-\infty}^{+\infty} N_s^2(E) \text{sech}^2 \left( \frac{E - E_F}{2k_B T} \right) dE. \quad (12)$$

If we use Eq. (7) for  $N_s(E)$  and the parameters derived from the Knight-shift fit, we find qualitatively poor agreement with experiment, in that  $(T_1 T)^{-1}$  is predicted to decrease monotonically with increasing  $T$  at  $P=6.9$  kbar. Alternatively, by increasing  $\Gamma$  and normalizing  $R_s$  and  $K_s$  separately [this accounts for different enhancement factors for  $K$  and  $(T_1 T)^{-1/2}$ ], we calculate the curves shown in Fig. 9. Again we followed the notation of JWWM in defining  $D'(T, P)$  by the relation

$$R(T, P) = r_s D'(T, P) + r_p (1 - \beta D'(T, P)), \quad (13)$$

where the terms have analogous meanings to their counterparts in the Knight-shift calculation. The agreement in this case, using the parameter values shown in Table II, is much poorer than for the Knight shift. This indicates that the model is less reliable for calculating  $T_1$  and that simple parameter adjustments cannot make up for shortcomings in the theory. Nevertheless, the capability of achieving a qualitative fit has significance regarding the slope of  $N(E)$ . In order for the initial change at  $T=0$  for  $K$  and  $(T_1 T)^{-1}$  to be of opposite sign, there must be structure in  $N(E)$  of width comparable to  $k_B T$ . This follows from the fact that  $K$  and  $(T_1 T)^{-1}$  are proportional to weighted averages of  $N_s(E)$  and  $N_s(E)^2$ , respectively [Eqs. (5) and (12)]. Of the three models we considered, only I exhibits this behavior.

We note that JWWM concluded that  $D'(T) = D(T)$ . Within our formulation, this can be rigorously correct only if  $N_s(E)$  is constant or a zero-based step function as, for example, in models II and III. Because of the temperature dependence of the Ga shift at high pressure, we believe the shape of  $N_s(E)$  to be more complicated. Unfortunately, at atmospheric pressure the range  $k_B T$  over which  $N_s(E)$  is averaged when hyperfine effects from the Ga  $s$  band first appear is much broader than the structure responsible for the low-temperature anomalies. The effects of this structure are therefore not directly observable in low-pressure experiments.

Since the band edges are smeared by adding Pd, the measured  $T_1$ 's exhibit a much slower variation with pressure in the doped samples (Fig. 4) than

TABLE II. Summary of parameters used in model calculation of  $D'(T, P)$ .

Model	A (eV)	B (eV/kbar)	C (eV/ $^{\circ}\text{K}$ )	$\chi$	$\beta$ (kbar) $^{-1}$	$f$	$\Gamma$ (eV)
I	0.012	-0.025	...	5.0	-0.2	0.35	0.0035

in pure AuGa<sub>2</sub>. As expected, Eq. (10) fails completely to account for the low-temperature pressure dependence of  $T_1$  in any of the alloys.

### C. Korringa Product

When a single hyperfine mechanism dominates, as for <sup>71</sup>Ga in AuGa<sub>2</sub> at high temperatures or pressures, the Korringa product, defined by  $K^2 T_1 T$ , is independent of the hyperfine coupling constant.<sup>27</sup> Moreover, in most metals it is temperature independent. However, if  $N(E)$  exhibits appreciable variation over an energy range  $k_B T$  around  $E_F$ , both  $K$  and  $T_1 T$  will be temperature dependent and, in general, so will  $K^2 T_1 T$ . Within our model the Korringa product for the  $s$ -hyperfine interaction is given by

$$K^2 T_1 T = \mathfrak{s} \frac{[\int N_s(E) f(1-f) dE]^2}{\int N_s(E)^2 f(1-f) dE}, \quad (14)$$

where  $\mathfrak{s}$  is a constant. Using Eq. (14) we find approximate experimental agreement for the temperature dependence of  $K^2 T_1 T$  at high pressure if the model parameters of Sec. IV B are used. However, the model is not capable of reproducing the pressure dependence of  $K^2 T_1 T$  at low temperature. These results are, of course, a direct consequence of the anomalous behavior of  $T_1 T$ .

Electron-electron interactions generally enhance  $K$  more than  $(T_1 T)^{-1/2}$ , so that one expects  $\mathfrak{K} \equiv \mathfrak{s} / (K^2 T_1 T) < 1$ . The limit  $\mathfrak{K} \rightarrow 0$  corresponds to a divergent static susceptibility.<sup>22,24</sup> Thus, the AuGa<sub>2</sub> results in Fig. 5 would seem to indicate an increasing exchange enhancement of the Ga  $s$ -band susceptibility above the transition. Such an effect cannot be understood on the basis of the postulated density-of-states functions. However, according to the band-structure calculation,<sup>13</sup> the Fermi-surface piece generated at the transition resembles intersecting spheroids which are very prolate. The magnetic response function for a metal with such a surface should approach that of a two-dimensional electron gas. For the two-dimensional case, the enhancements of  $K^2$  and  $(T_1 T)^{-1}$  cancel, making  $\mathfrak{K}$  unity.<sup>28</sup> As the Fermi level is lowered relative to the band edge, the sheets become more rounded and consequently more three dimensional in character. This change from two- to three-dimensional behavior would cause a decrease in  $\mathfrak{K}$ , as observed. If this conclusion is correct, the exchange enhancement at the transition may be quite large. Since this is not easily reconciled with the relatively high  $T_c$ , our interpretation must be considered speculative.

### D. Susceptibility

The observed decrease in the magnetic susceptibility<sup>1,3,12</sup> as  $T$  increases remains a puzzle. There exists considerable evidence that variations in the

susceptibility are not related to the density of Ga states at  $E_F$ . In addition to the dHvA work described earlier, we note that the low-temperature specific heat<sup>1</sup> of Pd-doped AuGa<sub>2</sub> increases as the Pd content increases. This indicates that the band-edge-Fermi-level interaction increases the density of states. The Pauli susceptibility should therefore increase, in contrast to the observed behavior of the bulk susceptibility. Although conduction-electron diamagnetism is possible, as noted by Warren *et al.*,<sup>3</sup> we expect the effective mass of electrons in the Ga  $s$  band to be high. Support for a large effective mass is provided by the failure to observe dHvA oscillations from the Fermi-surface piece created at the  $s$ -band intersection of  $E_F$ . We also note that the anomaly in  $\chi(T)$  for Pd-doped AuGa<sub>2</sub> occurs at about the same temperature as in pure AuGa<sub>2</sub>, in contrast to the <sup>71</sup>Ga Knight shift, which is already positive at low temperature.

We considered the possibility of Van Vleck susceptibility<sup>29</sup> variations as the Ga band intersects the Fermi level. Since  $d$  electrons produce a large orbital hyperfine interaction<sup>30</sup> and Au  $d$  states are admixed into the Ga  $s$  band, the Au Knight shift should increase markedly with pressure (but decrease with temperature as observed) if appreciable Van Vleck paramagnetism is present. The pressure independence of  $K$  for <sup>197</sup>Au suggests that this explanation is most likely incorrect. Therefore, while many of the anomalous properties of AuGa<sub>2</sub> can be accounted for satisfactorily by the band-structure-electron-transition picture, we can only surmise that the bulk susceptibility is a complicated sum of many contributions and is not amenable to our simple analysis.

### V. SUMMARY

We have presented nuclear-magnetic-resonance measurements of the Knight shift and spin-lattice relaxation time of <sup>71</sup>Ga in Au<sub>1-x</sub>Pd<sub>x</sub>Ga<sub>2</sub> for  $x = 0.0, 0.012, \text{ and } 0.026$  as a function of hydrostatic pressure to 8.4 kbar and temperature in the range 4–300 °K. The Knight shift for <sup>197</sup>Au in AuGa<sub>2</sub> was also measured as a function of pressure at 4 °K. Large increases for both the <sup>71</sup>Ga shift and relaxation rate in AuGa<sub>2</sub> were observed at 4 °K near 7-kbar pressure. However, the magnitudes of  $K$  and  $(T_1 T)^{-1}$  exhibited a decrease upon increasing  $T$  at high pressure. In contrast, the <sup>195</sup>Au shift showed both pressure and temperature independence. The Ga Korringa product ( $K^2 T_1 T$ ) was found to be both temperature and pressure dependent. Increases for  $K$  and  $(T_1 T)^{-1}$  were also found at 4 °K in Pd-doped AuGa<sub>2</sub>. Compared to pure AuGa<sub>2</sub>, the “turn on” occurred at lower pressures and was more gradual, and the magnitude of the effect was smaller.

We have interpreted these data in terms of a band-structure-electron-transition model which

we show can be put in semiquantitative terms at least for the Knight shift in  $\text{AuGa}_2$ . The electronic band structure of  $\text{AuGa}_2$  possesses the unusual property of having a flat Ga  $s$  band 10–15 meV below  $E_F$  at low temperature. This energy gap exhibits a pressure dependence such that  $E_F$  intersects the band edge near 7 kbar at 4 °K. This intersection gives rise to an "electron transition" involving creation of a second band-hole sheet of the Fermi surface with an associated high density of states.

The anomalous temperature dependence of the  $^{71}\text{Ga}$   $K$  and  $(T_1 T)^{-1}$  is produced by thermal averaging of the density of states at  $E_F$ . With increasing temperature, this effect increases  $K$  at low pressure, where  $E_F$  is above the Ga  $s$ -band edge and decreases  $K$  at high pressure, where  $E_F$  is below the edge. Although the available data do not rule out the possibility of an explicit temperature dependence in the band-edge location, as proposed by Warren *et al.*, we have shown that inclusion of such an effect does not improve agreement with experiment.

Addition of Pd to  $\text{AuGa}_2$  alters the response of the material to changes in pressure and temperature in a nonrigid-band manner. The Pd not only changes the positions of  $E_F$  and the Ga  $s$  band, but smears the edge appreciably compared to the size of the energy gap. This effect is evident in the resonance data for the Pd-doped samples, where the increases in  $K$  and  $(T_1 T)^{-1}$  with increasing pressure at 4 °K are less rapid and smaller in magnitude than for the pure compound.

Exchange enhancement is surprisingly large in  $\text{AuGa}_2$  when  $E_F$  intersects the Ga  $s$  band, as shown by a Korringa product ( $K^2 T_1 T$ ) which is five to ten times the free-electron value. The actual enhancement is uncertain, due to the changing topology of the Fermi surface as the Ga band intersects  $E_F$ .

#### ACKNOWLEDGMENTS

We wish to thank Dr. A. C. Switendick for many stimulating discussions. The samples were prepared by R. J. Baughman. The expert technical assistance of Barry Hansen, R. L. White, and D. C. Barham is acknowledged.

<sup>†</sup>Work supported by the U. S. Atomic Energy Commission.

<sup>1</sup>J. H. Wernick, A. Menth, T. H. Geballe, G. Hull, and J. P. Maita, *J. Phys. Chem. Solids* **30**, 1949 (1969).

<sup>2</sup>G. C. Carter, I. D. Weisman, L. H. Bennett, and R. E. Watson, *Phys. Rev. B* **5**, 3621 (1972).

<sup>3</sup>W. W. Warren, R. W. Shaw, A. Menth, F. J. DiSalvo, A. R. Storm, and J. H. Wernick, *Phys. Rev. B* **7**, 1247 (1973).

<sup>4</sup>J. T. Longo, P. A. Schroeder, and D. J. Sellmyer, *Phys. Rev.* **182**, 658 (1969).

<sup>5</sup>J. T. Longo, P. A. Schroeder, M. Springford, and J. R. Stockton, *Phys. Rev.* **187**, 1185 (1969).

<sup>6</sup>J. C. Abele, J. H. Brewer, and M. H. Halloran, *Solid State Commun.* **9**, 977 (1971).

<sup>7</sup>S. Hufner, J. H. Wernick, and K. W. West, *Solid State Commun.* **10**, 1013 (1972).

<sup>8</sup>L. R. Testardi, *Phys. Rev. B* **1**, 4851 (1970).

<sup>9</sup>J. E. Schirber, *Phys. Rev. B* **6**, 333 (1972).

<sup>10</sup>J. E. Schirber, *Phys. Rev. Lett.* **28**, 1127 (1972).

<sup>11</sup>T. F. Smith, R. N. Shelton, and J. E. Schirber, *Phys. Rev. B* **8**, 3479 (1973).

<sup>12</sup>V. Jaccarino, M. Weger, J. H. Wernick, and A. Menth, *Phys. Rev. Lett.* **21**, 1811 (1968).

<sup>13</sup>A. C. Switendick and A. Narath, *Phys. Rev. Lett.* **22**, 1423 (1969).

<sup>14</sup>J. P. Jan, W. B. Pearson, Y. Saito, M. Springford, and I. M. Templeton, *Philos. Mag.* **12**, 1271 (1965).

<sup>15</sup>J. E. Schirber and A. C. Switendick, *Solid State Commun.* **8**, 1383 (1970).

<sup>16</sup>I. M. Lifshitz, *Zh. Eksp. Teor. Fiz.* **38**, 1569 (1960) [*Sov. Phys.-JETP* **11**, 1130 (1960)].

<sup>17</sup>H. T. Weaver, J. E. Schirber, and A. Narath, in *Proceedings of the Thirteenth International Conference on Low Temperature*

*Physics, Boulder, Colo., 1972*, edited by R. H. Kropschot and K. D. Timmerhaus (University of Colorado Press, Boulder, Colo., 1973).

<sup>18</sup>A. Narath, *Phys. Rev.* **162**, 32C (1967).

<sup>19</sup>J. E. Schirber, *Cryogenics* **10**, 418 (1970).

<sup>20</sup>J. E. Schirber and D. W. Shanfeldt, *Rev. Sci. Instrum.* **39**, 270 (1968).

<sup>21</sup>G. Clark, *Rev. Sci. Instrum.* **35**, 316 (1964).

<sup>22</sup>T. Moriya, *J. Phys. Soc. Jap.* **18**, 516 (1963).

<sup>23</sup>C. P. Slichter, *Principles of Magnetic Resonance* (Harper & Row, New York, 1963), p. 96.

<sup>24</sup>A. Narath and H. T. Weaver, *Phys. Rev.* **175**, 375 (1968).

<sup>25</sup>In an earlier paper [*Phys. Rev. B* **1**, 974 (1970)] we measured the pressure dependence of the Knight shift and linewidth of  $^{133}\text{Cs}$  in cesium metal. These data included points taken in both liquid and solid helium. The smooth variation of the NMR parameters with pressure in this region, is good evidence that the pressure within the solid helium is hydrostatic. Furthermore a large body of de Haas-van Alphen data taken in both liquid and solid He on Bi, As, Sb, Cd, and Zn indicate that hydrostatic conditions are achieved in solid He even with these very anisotropic materials. See Ref. 19 and references therein.

<sup>26</sup>Reference 23, p. 124.

<sup>27</sup>Reference 23, p. 126.

<sup>28</sup>E. Ehrenfreund, E. F. Rybaczewski, A. F. Garito, and A. J. Heeger, *Phys. Rev. Lett.* **28**, 873 (1972).

<sup>29</sup>J. M. Ziman, *Principles of the Theory of Solids* (Cambridge U. P., New York, 1964), p. 284.

<sup>30</sup>A. J. Freeman and R. E. Watson, in *Magnetism*, edited by G. T. Rao and H. Suhl (Academic, New York, 1965), Vol. IIA, p. 267.